Syntheses and photophysical properties of a series of cation-sensitive polymethine and styryl dyes

Julia L. Bricks [a], Juri L. Slominskii [a], Margarita A. Kudinova [a], Alexei I. Tolmachev [a],
Knut Rurack [b,c,*], Ute Resch-Genger [b], Wolfgang Rettig [c]

[a] *Institute of Organic Chemistry, National Academy of Sciences, 5 Murmanskaya St., Kiev-94, UKR-253660, Ukraine*
[b] *I.3902, Federal Institute for Materials Research and Testing (BAM), Richard-Willstaetter Str. 11, D-12489 Berlin, Germany*
[c] *Institute of Physical and Theoretical Chemistry, Humboldt-Universität Berlin, Bunsenstr. 1, D-10117 Berlin, Germany*

Abstract

The syntheses and photophysical properties of 20 cation-sensitive fluoroionophores carrying the tetraoxa monoaza 15-crown-5 receptor are described and discussed. Whereas complexation induces only weak effects for the positively charged hemicyanine probes, the closely related styryl dyes show stronger changes in their photophysical properties upon cation binding in the analytically advantageous near-infrared (NIR) region. The strongest effects in both cation-induced spectral effects and complex stability constants are observed for the uncharged probes of styryl base-type, but these probes usually absorb and emit at shorter wavelengths in the UV/VIS region. For both styryl dyes and styryl bases, in some cases cation-induced fluorescence enhancement or quenching is found. © 2000 Elsevier Science S.A. All rights reserved.

Keywords: Fluorescence; Ionophores; Unsymmetrical cyanines; Styryl dyes; Styryl bases

1. Introduction

Chromo- and fluoroionophores, synthesized following a donor-π-system-acceptor design concept, play a major role in UV/VIS spectrophotometric and/or fluorometric ion analysis [1–4]. Such dyes usually consist of a macrocyclic (e.g., a monoaza or benzo crown ether) or acyclic ion-responsive receptor, often the electron donating moiety of the molecule, and a heterocyclic or polyaromatic moiety which can function as an electron-deficient acceptor [2,4]. Furthermore, donor and acceptor can be in direct electronic conjugation via an oligomethine π-system $-(CH=CH-)_n$ or a (elongated, for $n>1$) styrene-type π-system $-(CH=CH-)_n C_6H_4-$ and the acceptor moiety itself can (formally) be charged [5–12] or uncharged [1,13–20]. Dyes of the former type are mostly asymmetric hemicyanines and styryls, those of the latter type are often stilbene-analogue styryl bases. Based on their electronic properties, the spectroscopic behavior of the styryls and styryl bases is often determined by an intramolecular charge transfer (ICT) process accompanying optical excita-

tion [1,21]. Thus, especially in polar solvents, many of these dyes show characteristically broad and structureless absorption and emission spectra, the latter often being strongly Stokes-shifted. In contrast, the hemicyanines usually show the characteristic features of polymethine dyes, i.e., relatively narrow and structured spectra accompanied by a small Stokes shift [22–24].

Employing this design concept for chromo- or fluoroionophores, complexation of a cation to the donor part of an ICT compound or a polymethine dye leads to pronounced spectral shifts generating a signal change which can be exploited for ion sensing. Many such systems have been introduced in the literature so far [1–20] but until today the mechanisms governing the spectral changes (size and direction of the shift) as well as fluorescence enhancement or quenching upon complexation are only partly understood [2,3,25–29]. Thus, for a more systematic approach we synthesized a series of crowned dyes **1–14** (Scheme 1) including hemicyanine (**1–4**) and styryl dyes (**5–9**) as well as styryl bases (**10–14**), all of them equipped with the well-known receptor monoaza tetraoxa 15-crown-5 (A15C5) for alkali and alkaline-earth metal ions, and inves-

---

* Corresponding author.
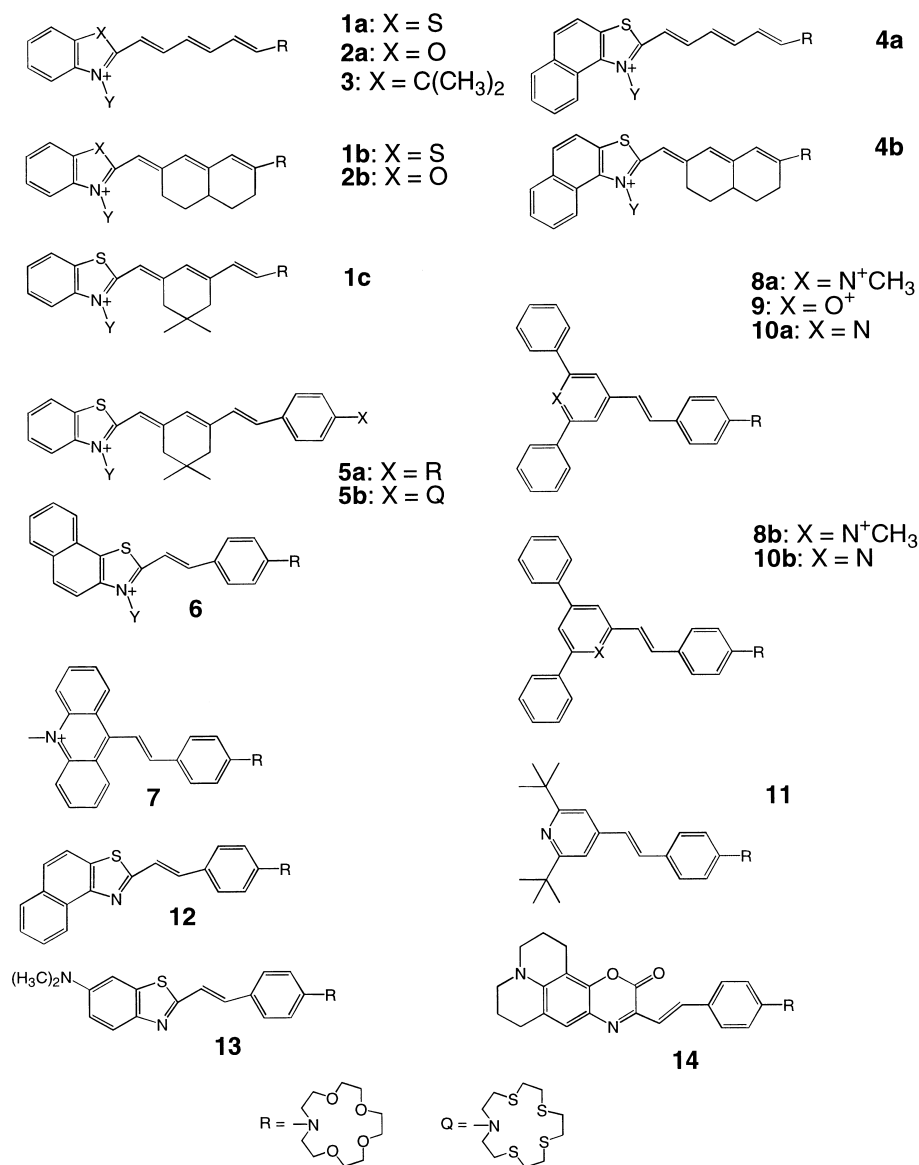
Scheme 1. Chemical structures of the dyes investigated (Y=C$_2$H$_5$ with the exception of **3**: Y=CH$_3$).

tigated their cation complexation properties in acetonitrile employing the calcium ion vicarious for the alkali and alkaline-earth metal ions.

2. Experimental details

2.1. Materials and apparatus

All chemicals for the synthesis were purchased from Merck. Calcium perchlorate (of highest purity available) and acetonitrile (spectrometric grade) were purchased from Aldrich. The salt was dried in a vacuum oven before use [30] and acetonitrile was distilled from CaH$_2$ prior to use.

The chemical structures of the dyes were confirmed by elemental analysis, ^{1}H NMR, and/or MS and their purity

was checked by reversed phase HPLC (HPLC set up from Merck–Hitachi; RP18 column; acetonitrile/water=75/25 as eluent) employing UV detection (UV detector from Knaur; fixed wavelength at 310 nm). NMR spectra were obtained with a 500 MHz NMR spectrometer Varian Unity$_{plus}$ 500. The mass spectra were recorded on a Finnigan MAT 95 spectrometer with an ESI-II/APCI-Source for electrospray ionization and the base peaks [M+Na]$^+$ were determined. The melting points (mp) measured with a digital melting point analyzer IA 9100 (Kleinfeld GmbH) are uncorrected.

2.2. Synthesis

The synthesis of the unbridged hexamethine hemicyanine dyes **1a**, **2a**, **3**, and **4a** containing heteromacrocycles as an

electron-accepting fragment followed the route of reacting the corresponding *N*-containing heterocyclic acetanilido hexatrienyl derivative (e.g., **A**) with monoaza tetraoxa 15-crown-5 in acetonitrile or *i*-propanol.

2.2.1. 2-[6-(1,4,7,10-Tetraoxa-13-azacyclopentadecan-13-yl)-hexa-1,3,5-trien-1-yl]-3-ethyl-naphtho[1,2-d]thiazolium perchlorate (4a)

2-[6-(*N*-Phenyl-acetamidyl)-hexa-1,3,5-trien-1-yl]-3-eth-yl-naphtho[1,2-d]thiazolium perchlorate (**A**) (0.001 mol) and 1,4,7,10-tetraoxa-13-azacyclopentadecane (0.0011 mol) were refluxed in acetonitrile (3 ml) for 5 min. After cool-ing, the reaction mixture was treated with absolute diethyl ether (50 ml) and the resinous precipitate was dissolved in acetonitrile (5 ml). Then a solution of sodium perchlorate (0.5 g) in acetonitrile (3 ml) was added and the product was precipitated with water. The precipitate was filtered and crystallized from methanol. Yield 36%. mp 192–194°C (from methanol), Elemental analysis (found: C, 57.00; H, 5.97; N, 4.75 Calc. for $C_{29}H_{37}N_2ClN_2O_8S$: C, 57.17; H, 6.12; N, 4.60). ^1H NMR (CDCl$_3$) δ (ppm): 1.452 (t, $J=7$ Hz, 3H, CH$_3$), 3.603–3.728 (m, 16H, –CH$_2$–O), 3.840 (t, unresolved, 4H, >N–CH$_2$–), 4.284–4.302 (q, unresolved, 2H, CH$_2$), 5.816 (t, unresolved, 1H, CH chain), 6.242 (d, $J=12.1$ Hz, 1H, CH chain), 6.416 (t, unresolved, 1H, CH chain), 7.285–7.813 (m, 9H, ArH and CH chain).

The hemicyanines **1a**, **2a**, and **3** were obtained in a similar way. Precipitation of **3** with water was followed by column chromatography on silica gel with chloro-form/ethanol (8/2) as eluent. After evaporation of the eluent, the product was dissolved in acetonitrile and pre-cipitated with ethyl acetate. Accordingly, **1a** and **2a** were precipitated with water as well and were then recrystallized from *i*-propanol. The resinous precipitates were dissolved in chloroform and treated with hexane to precipitate the hemicyanines.

2.2.2. 2-[6-(1,4,7,10-Tetraoxa-13-azacyclopentadecan-13-yl)-hexa-1,3,5-trien-1-yl]-3-ethyl-benzothiazolium perchlorate (1a)

Yield 42%. mp 88–90°C (from methanol), Elemental analysis (found: C, 60.28; H, 7.26; Cl, 5.70 Calc. for $C_{30}H_{43}ClN_2O_8S$: C, 60.55; H, 7.28; Cl, 5.95). ^1H NMR (CDCl$_3$) δ (ppm): 1.460 (t, $J=7$ Hz, 3H, CH$_3$), 3.613–3.731 (m, 16H, –CH$_2$–O), 3.836 (t, unresolved, 4H, >N–CH$_2$–), 4.282–4.297 (q, unresolved, 2H, CH$_2$), 5.846 (t, unresolved, 1H, CH chain), 6.227–6.252 (d, $J=12.5$ Hz, 1H, CH chain), 6.399 (t, unresolved, 1H, CH chain), 7.265–7.663 (m, 7H, ArH and CH chain).

2.2.3. 2-[6-(1,4,7,10-Tetraoxa-13-azacyclopentadecan-13-yl)-hexa-1,3,5-trien-1-yl]-3-ethyl-benzoxazolium perchlorate (2a)

Yield 51%. mp 59–61°C (from methanol), Elemen-tal analysis (found: C, 55.23; H, 6.42; N, 5.40 Calc. for $C_{25}H_{35}ClN_2O_9$: C, 55.29; H, 6.49; N, 5.16). ^1H NMR (CDCl$_3$) δ (ppm): 1.468 (t, $J=7.2$ Hz, 3H, CH$_3$), 3.600–3.729 (m, 16H, –CH$_2$–O), 3.840 (t, unresolved, 4H, >N–CH$_2$–), 4.276–4.293 (q, unresolved, 2H, CH$_2$), 5.842 (t, unresolved, 1H, CH chain), 6.223–6.250 (d, $J=12.5$ Hz, 1H, CH chain), 6.390 (t, unresolved, 1H, CH chain), 7.262–7.670 (m, 7H, ArH and CH chain).

2.2.4. 2-[6-(1,4,7,10-Tetraoxa-13-azacyclopentadecan-13-yl)-hexa-1,3,5-trien-1-yl]-1,3,3-trimethyl-3H-2-indolium perchlorate (3)

Yield 65%. mp 68–70°C (from acetonitrile). Elemen-tal analysis (found: C, 58.30; H, 7.13; N, 6.30 Calc. for $C_{27}H_{39}ClN_2O_8$: C, 58.42; H, 7.08; N, 6.38). ^1H NMR (CDCl$_3$) δ (ppm): 1.643 (s, 6H, C(CH$_3$)$_2$), 3.467 (s, 3H, NCH$_3$), 3.611–3.690 (m, 16H, –CH$_2$–O), 3.796–3.820 (t, $J=6.4$ Hz, 4H, >N–CH$_2$–), 5.841–5.868 (d, $J=13.4$ Hz, 1H, CH chain), 6.043–6.092 (t, $J=12.2$ Hz, 1H, CH chain), 6.431–6.381 (t, $J=12.5$ Hz, 1H, CH chain), 6.969–6.985 (d, $J=8.0$ Hz, 2H, ArH), 7.135–7.164 (t, $J=7.4$ Hz, 1H, ArH), 7.266–7.339 (m, 2H, ArH and CH chain), 7.712–7.764 (t, $J=12.8$ Hz, 1H, CH chain), 7.960–7.983 (d, $J=11.6$ Hz, 1H, CH chain).

The hemicyanines with four sterically fixed hexame-thine bonds, **1b**, **2b**, and **4b**, were synthesized by conden-sation of the respective precursor salt, e.g., 1-ethyl-2-methyl-benzothiazolium-toluene-4-sulphonate (**B**) with 1,4,5,8-tetrahydro-2,7-dimethoxynaphthalene (**C**) followed by nucleophilic substitution of the terminal methoxy group of the intermediate (e.g., **D**) by monoaza tetraoxa 15-crown-5 [31].

2.2.5. 2-[7-(1,4,7,10-tetraoxa-13-azacyclopentadecan-13-yl)-4,4a,5,6-tetrahydro-2(3H)naphthalenylidene]-3-ethyl-benzothiazolium perchlorate (1b)

D (0.001 mol) and 1,4,7,10-tetraoxa-13-azacyclopenta-decane (0.0014 mol) were refluxed in acetonitrile (3 ml) for 7 min. The reaction mixture was diluted with dry diethyl ether (50 ml) and the resinous residue was dissolved in acetonitrile and filtered. The dye precipitated with diethyl ether was dissolved in chloroform and again precipitated with hexane. Yield 49%. mp 91–93°C (from methanol). Elemental analysis (found: C, 60.67; H, 6.84; Cl, 5.82 Calc. for $C_{30}H_{41}ClN_2O_8S$: C, 60.75; H, 6.96; Cl, 5.97). ^1H NMR (CDCl$_3$) δ (ppm): 1.243–1.289 (t, $J=6.8$ Hz, 3H, CH$_3$), 1.389–1.432 (m, 2H, C–CH$_2$), 1.992–2.040 (m, 2H, C–CH$_2$), 2.504–2.898 (m, 5H, –CH(CH$_2$)$_2$), 3.610–3.742 (m, 16H, –CH$_2$–O), 3.828 (t, unresolved, 4H, >N–CH$_2$–), 4.279–4.304 (q, unresolved, 2H, CH$_2$), 5.990 (s, 1H, CH chain), 6.072 (s, 1H, CH chain), 6.380 (s, 1H, CH chain), 7.249–7.298 (t, $J=7.4$ Hz, 1H, ArH), 7.462–7.513 (t, $J=7.0$ Hz, 1H, ArH), 7.557–7.583 (d, $J=8.0$ Hz, 1H, ArH), 7.846–7.869 (d, $J=7.7$ Hz, 1H, ArH).

2.2.6. 2-[7-(1,4,7,10-tetraoxa-13-azacyclopentadecan-13-yl)-4,4a,5,6-tetrahydro-2(3H)naphthalenylidene]-3-ethyl-benzoxazolium perchlorate (2b)

Yield 28%. mp 98–100°C (from methanol). Elemental analysis (found: C, 59.10; H, 6.68; N, 4.53 Calc. for $C_{20}H_{41}ClN_2O_9$: C, 59.15; H, 6.78; N, 4.50). ^{1}H NMR (CDCl$_3$) δ (ppm): 1.268–1.299 (t, J=7.0 Hz, 3H, CH$_3$), 1.384–1.430 (m, 2H, C–CH$_2$), 1.996–2.022 (m, 2H, C–CH$_2$), 2.444–3.018 (m, 5H, –CH(CH$_2$)$_2$), 3.614–3.738 (m, 16H, –CH$_2$–O), 3.800 (t, unresolved, 4H, >N–CH$_2$–), 4.120–4.160 (q, unresolved, 2H, CH$_2$), 5.592 (s, 1H, CH chain), 6.034 (s, 1H, CH chain), 6.580 (s, 1H, CH chain), 7.229–7.288 (t, J=7.4 Hz, 1H, ArH), 7.362–7.410 (t, J=7.0 Hz, 1H, ArH), 7.607–7.623 (d, J=8.0 Hz, 1H, ArH), 7.849 (broad, 1H, ArH).

2.2.7. 2-[7-(1,4,7,10-tetraoxa-13-azacyclopentadecan-13-yl)-4,4a,5,6-tetrahydro-2(3H)naphthalenylidene]-3-ethyl-naphtho[1,2-d]thiazolium perchlorate (4b)

In the case of **4b**, for the last step, i.e., condensation of chromophore and receptor precursor, pyridine (3 ml) was used. Yield 30%. mp 182–183°C (from chloroform). Elemental analysis (found: C, 61.37; H, 5.90; N, 4.05 Calc. for $C_{44}H_{43}ClN_2O_8S$: C, 60.47; H, 6.42; N, 4.15). ^{1}H NMR (DMSO-d$_6$) δ (ppm): 1.376–1.460 (m, 2H, C–CH$_2$), 1.641–1.688 (t, J=7.1 Hz, 3H, CH$_3$), 2.005 (t, unresolved, 2H, C–CH$_2$), 2.330–2.930 (m, 5H, –CH(CH$_2$)$_2$), 3.537–3.621 (m, 12H, –CH$_2$–O), 3.753 (broad, 8H, >N–(CH$_2$)$_2$–), 4.717–4.816 (q, unresolved, 2H, CH$_2$), 5.879 (s, 1H, CH chain), 6.343 (s, 1H, CH chain), 6.429 (s, 1H, CH chain), 7.646–7.695 (t, J=7.4 Hz, 1H, ArH), 7.726–7.773 (t, J=7.0 Hz, 1H, ArH), 7.908–7.937 (d, J=8.8 Hz, 1H, ArH), 7.997–8.026 (d, J=8.8 Hz, 1H, ArH), 8.117–8.143 (d, J=7.8 Hz, 1H, ArH), 8.471–8.500 (d, J=8.7 Hz, 1H, ArH).

2.2.8. 2-[(7-Methoxy-4,4a,5,6-tetrahydro-2(3H)naphthalenylidene)methyl]-3-ethyl benzothiazolium perchlorate (D)

1-Ethyl-2-methyl-benzothiazolium-*p*-toluene-4-sulphonate **B** (1.6 g, 0.0054 mol) and 2,7-dimethoxy-1,4,5,8-tetrahydronaphthalene **C** (1.4 g, 0.007 mol) were reacted at 115–117°C for 15 min. The product was treated with dry diethyl ether (twice 10 ml) and dissolved in ethanol. **D** was precipitated with an aqueous solution of sodium perchlorate and crystallized from *i*-propanol. Yield 61%. mp 210–212°C (from methanol). Elemental analysis (found: C, 59.70; H, 5.78; N, 3.41 Calc. for $C_{21}H_{24}ClNO_6$: C, 59.78; H, 5.73; N, 3.32).

Starting with the corresponding benzothiazole acetanilido hexatrienyl derivative the hemicyanine **1c** carrying a *neo*-pentylene bridge in β- and δ-position was obtained by condensation with the secondary amine receptor unit.

2.2.9. 2-[6-(1,4,7,10-Tetraoxa-13-azacyclopentadecan-13-yl)-2,4-(β,β-dimethyl-trimethylene)hexa-1,3,5-trien-1-yl]-3-ethylbenzothiazolium perchlorate (1c)

The mixture of acetanilidohexatrienyl-substituted benzothiazolium perchlorate (0.005 mol) and monoaza 15-crown-5 was refluxed in acetonitrile (3 ml) for 7 min. When cooled down, the reaction mixture is poured into dry diethyl ether (100 ml). The resulting resinous precipitate was dissolved in chloroform (15 ml). The solution was filtered and evaporated to dryness in vacuum. The precipitate was dissolved in chloroform (5 ml) and the dye was precipitated with hexane (100 ml). Yield 42%, mp 88–90°C (from methanol). Elemental analysis (found: C, 60.28; H, 7.26; Cl, 5.70 Calc. for $C_{30}H_{43}ClN_2O_8S$: C, 60,55; H, 7.28; Cl, 5.95). ^{1}H NMR (DMSO-d$_6$) δ (ppm): 1.041 (s, 6H, C(CH$_3$)$_2$), 1.240–1.332 (t, J=7.2 Hz, 3H, CH$_3$), 2.494 (s, 2H, CH$_2$ bridge), 2.594 (s, 2H, CH$_2$ bridge), 3.521–3.609 (m, 12H, –CH$_2$–), 3.694–3.731 (m, 8H, >N–(CH$_2$)$_2$–), 4.397–4.465 (q, J=6.8 Hz, 2H, CH$_2$), 5.801–5.841 and 7.865–7.905 (2×d, J=12.2 Hz, 2H, CH=CH), 6.382 (s, 1H, CH chain), 6.564 (s, 1H, CH chain), 7.378–7.428 (m, 1H, ArH), 7.562–7.617 (m, 1H, ArH), 7.742–7.769 (d, J=8.3 Hz, 1H, ArH), 8.010–8.036 (d, J=7.8 Hz, 1H, ArH).

For the styryl probes **5a**, **5b**, and **6**, the precursor compounds 1-ethyl-2-methyl-benzothiazolium perchlorate and its bridged tetramethine derivative were reacted with 4-(4,7,10,13-tetra-X-1-azacyclopentadecyl)benzaldehyde (with X=oxa or thia) in dimethylacetamide employing piperidine as catalyst. The synthesis of the heterocyclic precursors was described [32,33]. **7** and **9** were obtained from 9,10-dimethylacridinium methylsulfate and 2,6-diphenyl-4-methylpyrylium tetrafluoroborate and the crowned benzaldehyde. In the case of **8a** and **8b**, **9** was reacted with methylamine in acetonitrile [34]. The pyrylium precursor salts were synthesized in analogy to the methods described in [35] (2,6-diphenyl- and 2,4-diphenyl-4-methylpyrylium salts) and [36] (2,6-di(t-butyl)-4-methylpyrylium perchlorate).

2.2.10. 2-(5,5-Dimethyl-3-{2-[4-(1,4,7,10-tetraoxa-13-aza-cyclopentadec-13-yl)-phenyl]-vinyl}-cyclohex-2-enylidene-methyl)-3-ethyl-benzothiazolium iodide (5a)

Yield 43%. mp 254–256°C (from methanol). MS (*m/z*: 603.3282 [M-A]. Calc. for $C_{36}H_{47}N_2O_4S$: 603.3257). Elemental analysis (found: C, 59.28; H, 6.42; N, 3.85 Calc. for $C_{36}H_{47}N_2O_4S$: C, 59.17; H, 6.49; N, 3.83). ^{1}H NMR (CDCl$_3$) δ (ppm): 1.144 (s, 6H, (CH$_3$)$_2$C), 1.609–1.638 (t, J=7.3 Hz, 3H, CH$_3$), 2.465 (s, 2H, CH$_2$ bridge,), 2.685 (s, 2H, CH$_2$ bridge), 3.636–3.685 (m, 16 H, –CH$_2$–O), 3.770–3.794 (t, J=6.1 Hz, 4H, >N–CH$_2$–, 5.083–5.120 (q, unresolved, 2H, CH$_2$), 6.643–6.661 (d, J=9.0 Hz, 2H, 2 PhH), 7.413–7.432 (d, J=9.0 Hz, 2H, 2 PhH), 6.806 (s, 1H, H-α), 6.924–6.955 and 7.000–7.032 (2×d, J=15.9 Hz, 2H, –CH=CH–), 7.524 (s, 1H, H-γ), 7.577–7.762 (m, 2H, CH-5,6 (benzothiazole)), 7.903–7.920 and 8.023–8.040 (2 d, J=8.4 Hz, 2H, CH-4,7 (benzothiazole)).

2.2.11. 2-(5,5-Dimethyl-3-{2-[4-(1,4,7,10-tetrathia-13-aza-cyclopentadec-13-yl)-phenyl]-vinyl}-cyclohex-2-enylidenemethyl)-3-ethyl-benzothiazolium iodide (**5b**)

Yield 26%. mp 265.6–266.7°C (from acetonitrile). MS (*m/z*: 667.2343 [M-A]. Calc. for $C_{36}H_{47}N_2S_5$: 667.2343). Elemental analysis (found: C, 56.15; H, 6.02; N, 3.87 Calc. for $C_{36}H_{47}ClN_2O_4S_5$: C, 56.33; H, 6.17; N, 3.65). ^{1}H NMR (CDCl$_3$) δ (ppm): 1.053–1.148 (t, 6H, C(CH$_3$)$_2$), 1.403–1.452 (t, J=7.3 Hz, 3H, CH$_3$), 2.526 (s, 2H, CH$_2$-4), 2.720–2.808 (m, 18H, CH$_2$-6, CH$_2$–S), 3.598–3.620 (t, unresolved, 4H, >N–CH$_2$–), 4.788–4.812 (q, unresolved, 2H, CH$_2$), 6.665–6.695 (d, J=9.2 Hz, 2H, 2 PhH), 7.481–7.510 (d, J=8.5 Hz, 2H, 2 PhH), 6.866 (s, 1H, H-α), 6.899–6.952 and 7.098–7.151 (2×d, J=15.9 Hz, 2H, –CH=CH–), 7.268 (s, 1H, H-γ), 7.683–7.863 (m, 2H, CH-5,6 (benzothiazole)), 8.198–8.227 and 8.361–8.388 (2 d, J_1=8.8 Hz, J_2=8.1 Hz, 2H, CH-4,7 (benzothiazole)).

2.2.12. 3-Ethyl-2-{2-[4-(1,4,7,10-tetraoxa-13-aza-cyclopentadec-13-yl)phenyl]-vinyl}-naphtha[2,1-d]thiazolium perchlorate (**6**)

A solution of 0.198 g (0.5 mmol) 2-methyl-3-ethyl-naphtho[2,1-d]thiazolium *p*-tolylsulphonate and 0.162 g 4-*N*-(1,4,7,10-tetraoxa-13-azacyclopentadecyl) benzaldehyde in 3 ml dimethylacetamide was heated for 30 min at 120°C. After cooling down, 50 ml diethyl ether were added. The resulting oil was dissolved in 5 ml methanol and a solution of 0.5 g NaClO$_4$ in 5 ml water was added. The solid dye perchlorate was filtered off, washed with water, methanol, and diethyl ether. Yield 42%. mp 164–165°C (from ethanol). MS (*m/z*: 533.2474 [M-A]. Calc. for $C_{31}H_{37}N_2O_4S$: 533.2475). Elemental analysis (found: C, 58.92; H, 5.68; N, 4.54 Calc. for $C_{31}H_{37}ClN_2O_8S$: C, 58.80; H, 5.89; N, 4.42). ^{1}H NMR (DMSO-d$_6$) δ (ppm): 1.467–1.514 (t, J=7 Hz, 3H, CH$_3$), 3.516–3.592 (m, 12H, –CH$_2$–O), 3.692–3.703 (m, 8H, N(CH$_2$–CH$_2$)$_2$), 4.931–4.955 (q, unresolved, 2H, CH$_2$), 6.830–6.859 (d, J=8.8 Hz, 2H, PhH), 7.668–7.719 and 8.114–8.164 (2×d, J=15.4 Hz, 2H, –CH=CH–), 7.763–7.917 (m, 4H, ArH), 8.185–8.256 (m, 3H, ArH), 8.336–8.366 (d, J=9.3 Hz, 1H, ArH).

2.2.13. 10-Methyl-9-{2-[4-(1,4,7,10-tetraoxa-13-aza-cyclopentadec-13-yl)-phenyl]vinyl}acridinium perchlorate (**7**)

9,10-dimethylacridinium methylsulfate was obtained by reacting 9-methylacridine with dimethylsulfate in dimethylacetamide. Then a solution of 0.156 g (0.5 mmol) 9,10-dimethylacridinium methylsulfate and 0.162 g 4-*N*-(1,4,7,10-tetraoxa-13-aza-cyclopentadecyl)benzaldehyde in 3 ml acetic anhydride was heated for 30 min at 100°C. After cooling down, 50 ml diethyl ether were added. The resulting oil was dissolved in 5 ml methanol and a solution of 0.5 g NaClO$_4$ in 5 ml water was added. The solid dye perchlorate was filtered off, washed with water, methanol, and diethyl ether. Yield 97%. mp 145–147°C (from ethanol).

Elemental analysis (found: C, 62.45; H, 6.16; N, 4.48 Calc. For $C_{32}H_{37}ClN_2O_8$: C, 62.69; H, 6.08; N, 4.57). ^{1}H NMR (DMSO-d$_6$) δ (ppm): 3.516 (s, 4H, CH$_2$-e), 3.554–3.584 (m, 8H, –CH$_2$–O), 3.670–3.717 (m, 8H, >N–CH$_2$–CH$_2$–), 4.627 (s, 3H, N–CH$_3$), 6.830 (d, J=9.2 Hz, 2H, CH-3′,5′), 7.426 and 8.392 (2×d, J=15.6 Hz, 2H, –CH=CH–), 7.859–8.834 (m, 10H, ArH).

2.2.14. 1-Methyl-2,6-diphenyl-4-{2-[4-(1,4,7,10-tetraoxa-13-aza-cyclopentadec-13-yl)-phenyl]vinyl} pyrydinium perchlorate (**8a**)

A solution of 0.25 mmol **9** and 2.7 mmol methylamine (methanol solution) in 6 ml acetonitrile was heated at 80°C for 1 h. The dye was precipitated by adding 1 ml 5% HClO$_4$, filtered off, and washed with water. Yield 80%. mp 164–168°C (from ethanol/water 1:1). MS (*m/z*: 565.30663 [M-A]. Calc. for $C_{36}H_{41}N_2O_4$: 565.734). Elemental analysis (found: C, 64.82; H, 6.15; N; 4.32 Calc. for $C_{36}H_{41}ClN_2O_8$: C, 65.00; H, 6.21; N, 4.21). ^{1}H NMR (DMSO-d$_6$) δ (ppm): 3.503 (s, 4H, CH$_2$-e), 3.628 (s, 3H, CH$_3$), 3.596–3.662 (d×d, J=5.2 Hz, 4H, CH$_2$-a,b), 3.548 (s, unresolved, 4H, CH$_2$-c,d), 6.764 (d, J=8.8 Hz, 2H, CH-8), 7.194 (d, J=16 Hz, 1H, CH-4), 7.551 (d, J=8.8 Hz, 2H, CH-7), 7.672–7.808 (m, 10H, CH-o,m,p), 8.040 (s, 2H, CH-2), 8.084 (d, J=16 Hz, 1H, CH-5).

2.2.15. 1-Methyl-2,4-diphenyl-6-{2-[4-(1,4,7,10-tetraoxa-13-aza-cyclopentadec-13-yl)-phenyl]vinyl} pyrydinium perchlorate (**8b**)

8b was obtained using the procedure described above for **8a**. Yield 85%. mp 152–153°C (from ethanol/water 1:1). Elemental analysis (found: C, 64.92; H, 6.25; N, 3.95 Calc. for $C_{36}H_{41}ClN_2O_8$: C,65.00; H, 6.21; N, 4.21). ^{1}H NMR (CDCl$_3$) δ (ppm): 3.58–3.61 (m, 12H, –CH$_2$–O), 3.718 (m, 4H, >N–CH$_2$–), 3.995 (s, 3H, NCH$_3$), 6.622 (d, J=9.0 Hz, 2H, PhH), 7.126 and 7.782 (2×d, J=16.2 Hz, 2H, –CH=CH–), 7.465–7.703 (m, 10H, ArH), 7.905 (s, 2H, H-β pyridine), 8.101 (d, J=9.0 Hz, 2H, PhH).

2.2.16. 2,6-Diphenyl-4-{2-[4-(1,4,7,10-tetraoxa-13-aza-cyclopentadec-13-yl)-phenyl]vinyl}pyrylium tetrafluoroborate (**9**)

The mixture of 1 mmol 2,6-diphenyl-4-methylpyrylium tetrafluoroborate and 1 mmol 4-*N*-(1,4,7,10-tetraoxa-13-azacyclopentadecyl)benzaldehyde was heated at 120–125°C for 1 h. After cooling the dye was filtered off, washed with acetic acid and diethyl ether. Yield 48%. mp 237–238°C (from acetonitrile). MS (*m/z*: 552.244 [M-A]. Calc. for $C_{35}H_{38}NO_5$: 552.275). Elemental analysis (found: C, 65.92; H, 5.85; F, 11.67 Calc. for $C_{35}H_{38}BF_4NO_5$: C, 65.74; H, 5.99; F, 11.88). ^{1}H NMR (DMSO-d$_6$) δ (ppm): 3.519 (s, 4H, –CH$_2$–O (e)), 3.558–3.602 (m, 8H, –CH$_2$–O (c+d)), 3.728 (s, 8H, –NCH$_2$–CH$_2$– (a+b)), 6.920–6.943 (d, J=7 Hz, 2H, CH-8), 7.225–7.263 (d, J=11.5 Hz, 1H, CH-4), 7.686–7.774 (m, 8H, CH-7,m,p), 8.258–8.278 (t,

unresolved, 4H, CH-o), 8.419 (s, 2H, CH-2), 8.585–8.623 (d, $J=11.4$ Hz, 1H, CH-5).

10a, **10b**, and **11** were obtained in an analogous way by heating the corresponding pyrylium dyes with aqueous ammonia in pyridine. For the other styryl bases, in principle, a procedure similar to that for **7** and **9** was employed. **12**, **13**, and **14** were obtained by condensation of 2-methyl-naphto[1,2-a]thiazole, 6-dimethylamino-2-methyl-benzothiazole, and the corresponding oxazinone precursor with the A15C5-substituted benzaldehyde.

2.2.17. 2,6-Diphenyl-4-[2-[4-(1,4,7,10-tetraoxa-13-aza-cyclopentadec-13-yl)-phenyl]vinyl]pyridine (10a)

1.5 ml 25% aqueous NH_3 were added to a solution of 0.5 mmol **9** in 5 ml pyridine heated at 100°C for 2 h. The solid precipitated was filtered off, washed with water and ethanol and purified by column chromatography (silica/CH_2Cl_2). Yield 30%. mp 174–175°C (from acetonitrile). MS (m/z: 573.3540 [M+Na]$^+$. Calc. for $C_{35}H_{38}N_2O_4Na$: 573.699). Elemental analysis (found: C, 76.50; H, 6.92; N, 5.22 Calc. for $C_{35}H_{38}N_2O_4$: C, 76.33; H, 6.95; N, 5.09). ^{1}H NMR (CDCl$_3$) δ (ppm): 3.591–3.652 (m, 16H, –CH_2–O), 3.734 (t, $J=5.7$ Hz, 4H, >N–CH_2–), 6.63 (d, $J=8.7$ Hz, 2H, PhH), 6.89 and 7.31 (2×d, $J=16.2$ Hz, 2H, –CH=CH–), 7.38–7.48 (m, 10H, ArH), 7.68 (s, 2H, H-β pyridine).

2.2.18. 2,4-Diphenyl-6-[2-[4-(1,4,7,10-tetraoxa-13-aza-cyclopentadec-13-yl)-phenyl]vinyl]pyridine (10b)

10b was obtained using the procedure described above for **10a**. Yield 42%. mp 166–167°C (from acetonitrile). MS (m/z: 573.3540 [M+Na]$^+$. Calc. for $C_{35}H_{38}N_2O_4Na$: 573.699). Elemental analysis (found: C, 76.20; H, 7.00; N, 5.17 Calc. for $C_{35}H_{38}N_2O_4$: C, 76.33; H, 6.95; N, 5.09). ^{1}H NMR (CDCl$_3$) δ (ppm): 3.578–3.610 (m, 16H, –CH_2–O), 3.723 (t, $J=5.8$ Hz, 4H, >N–CH_2–), 6.615 (d, $J=8.7$ Hz, 2H, PhH), 7.048 (d, $J=16.2$ Hz, 1H, –CH=CH–), 7.371–7.529 (m, 9H, ArH and H-β pyridine), 7.659–7.713 (m, 4H, ArH and –CH=CH–), 8.068 (d, $J=8.4$ Hz, 2H, PhH).

2.2.19. 2,6-Di-t-butyl-4-{2-[4-(1,4,7,10-tetraoxa-13-aza-cyclopentadec-13-yl)-phenyl]-vinyl}-pyridine (11)

11 was obtained using the procedure described above for **10a**. Yield 24%. mp 114–115°C (from acetonitrile). MS (m/z: 533.3355 [M+Na]$^+$. Calc. for $C_{31}H_{46}N_2O_4Na$: 533.719). Elemental analysis (found: C, 73.03; H, 9.00; N, 5.55 Calc. for $C_{31}H_{46}N_2O_4$: C, 72.91; H, 9.08; N, 5.48). ^{1}H NMR (CDCl$_3$) δ (ppm): 1.30 (s, 18H, t-Bu-H), 3.54–3.65 (m, 16H, –CH_2–O), 3.71 (t, $J=5.7$ Hz, 4H, >N–CH_2–), 6.59 (d, $J=8.7$ Hz, 2H, PhH), 6.76 and 7.11 (2×d, $J=16.5$ Hz, 2H, –CH=CH–), 7.07 (s, 2H, H-β pyridine), 7.34 (d, $J=8.7$ Hz, 2H, ArH).

2.2.20. 2-{2-[4-(1,4,7,10-Tetraoxa-13-azacyclopentadec-13-yl)phenyl]-vinyl}-naphtha[1,2-a]thiazole (12)

A mixture of 0.42 g (2 mmol) 2-methylnaphto[1,2-a]-thiazole and 0.76 g (2.4 mmol) 4-N-(1,4,7,10-tetraoxa-13-azacyclopentadecyl)-benzaldehyde was dissolved in 2 ml DMSO. 0.25 g powdered KOH were added and the resulting mixture was heated at 70°C for 2 h. The reaction mixture was poured into 50 ml water. The solid precipitate was filtered off and purified by column chromatography (Al$_2$O$_3$/benzene). Yield 16%. mp 109–110°C (from i-propanol). MS (m/z: 505.2155 [M+H]$^+$. Calc. for $C_{29}H_{33}N_2O_4S$: 505.2161). Elemental analysis (found: C, 68.78; H, 6.49; N, 5.45 Calc. for $C_{29}H_{32}N_2O_4S$: C, 69.02; H, 6.32; N, 5.55). ^{1}H NMR (CDCl$_3$) δ (ppm): 3.634–3.688 (m, 16H, –CH_2–O), 3.773–3.797 (t, $J=6.2$ Hz, 4H, >N–CH_2–), 6.677–6.695 (d, $J=8.9$ Hz, 2H, PhH), 7.298–7.331 and 7.466–7.497 (2×d, $J=16$ Hz, 2H, –CH=CH–), 7.540–7.572 (m, 1H, ArH), 7.636–7.655 (m, 1H, ArH), 7.741–7.759 (d, $J=8.7$ Hz, 1H, ArH), 7.839–7.857 (d, $J=8.7$ Hz, 1H, ArH), 7.914–7.931 (d, $J=8.1$ Hz, 1H, ArH), 8.791–8.808 (d, $J=8.1$ Hz, 1H, ArH).

2.2.21. 2-[2-(4-(1,4,7,10-Tetraoxa-13-azacyclopentadec-13-yl)-phenyl)vinyl]-6-dimethylaminobenzothiazol (13)

A mixture of 0.384 g (2 mmol) 6-dimethylamino-2-methylbenzothiazole, 0.64 g (2 mmol) 4-N-(1,4,7,10-tetra-oxa-13-aza-cyclopentadecyl)benzaldehyde and 0.25 g powdered KOH was heated in 3 ml DMSO at 80–90°C for 2 h. The reaction mixture was poured into 50 ml water and extracted by chloroform (3 ml×50 ml). The solvent was evaporated and the residue was recrystallized from acetonitrile. Yield 18%. mp 126–127°C (from acetonitrile). MS (m/z: 498.2438 [M+H]$^+$. Calc. for $C_{27}H_{36}N_3O_4S$: 498.2426). Elemental analysis (found: C, 65.44; H, 7.05; N, 8.68 Calc. for $C_{27}H_{35}N_3O_4S$: C, 65.16; H, 7.09; N, 8.44). ^{1}H NMR (CDCl$_3$) δ (ppm): 3.016 (s, 6H, N(CH$_3$)$_2$), 3.630–3.769 (m, 20H, –CH_2–O), 6.657 and 7.414 (2×d, $J=8.7$ Hz, 4H, PhH), 6.888–7.752 (m, 4H, ArH), 7.140 and 7.265 (2×d, $J=16.1$ Hz, 2H, –CH=CH–).

2.2.22. (6,7,9,10-Tetrahydro-2H,8H,11H-(1)benzo[6,7,8-ij]-quinolyzino-3-{2-[4-(1,4,7,10-tetraoxa-13-azacyclo-pentadec-13-yl)-phenyl]vinyl}1,4-oxazin-2-on) (14)

14 was obtained from 0.256 g (0.001 mol) oxazinone **E**, 0.225 g (0.0015 mol) anhydrous sodium iodide and 0.485 g (0.0015 mol) 4-N-(1,4,7,10-tetraoxa-13-azacyclopentadecyl) benzaldehyde. This mixture was heated in 2 ml acetic anhydride at 140°C for 6 h. After cooling down, a mixture of methylene chloride and water (1:1) was added. The organic layer was separated and washed with water. After evaporation of the solvent, the resulting product was purified by column chromatography (silica gel/chloroform). Yield 14%. mp 115–116°C. MS (m/z: 562.2943 [M+H]$^+$. Calc. for $C_{32}H_{40}N_3O_6$: 562.2917). Elemental analysis (found: C, 68.34; H, 7.13; N, 7.25 Calc. for $C_{32}H_{39}N_3O_6$: C, 68.43; H, 7.00; N, 7.48). ^{1}H NMR (CDCl$_3$) δ (ppm): 1.861 (m,

4H, Ar-CH$_2$), 2.74 (m, 4H, –CH$_2$–), 3.50–3.62 (m, 16H, –CH$_2$–O), 3.72 (t, J=5.6 Hz, 4H, >N–CH$_2$–), 6.56 and 7.36 (2×d, J=8.7 Hz, 4H, PhH), 6.82 and 7.64 (2×d, J=15.9 Hz, 2H, –CH=CH–), 7.10 (s, 1H, ArH).

The oxazinone precursor **E** was synthesized starting with 8-hydroxyjulolidine. A solution of 1.8 g (0.026 mol) sodium nitrite in 3 ml water was added dropwise to a mixture of 4.7 g (0.025 mol) 8-hydroxyjulolidine and 30 g ice in 30 ml concentrated HCl and the reaction mixture was stirred at 5–8°C for 2 h. The resulting salt was filtered off and treated with a solution of sodium acetate. The product was crystallized from ethanol/water (1:5). Yield 40%. mp 140°C. 8-Hydroxy-9-nitroso-julolidine was used without analysis for further transformations, i.e., a mixture of 2.0 g (0.009 mol) 8-hydroxy-9-nitroso-julolidine and 1.5 g Ni–Raney catalyst in 120 ml ethanol was treated with H$_2$ for 2 h. After addition of 1.8 g (1.015 mol) ethylpuruate (under Ar) the reaction mixture was refluxed for 2 h yielding **E**. Evaporation of the solvent was followed by recrystallization of the solid from ethanol. Yield 54%. mp 135–136°C. Elemental analysis (found: C, 70.23; H, 6.55; N, 10.89 Calc. for C$_{15}$H$_{16}$N$_2$O$_2$:%: C, 70.29; H, 6.29; N, 10.93). ^{1}H NMR (CDCl$_3$) δ (ppm): 1.91 (m, 4H, Ar-CH$_2$), 2.39 (s, 3H, CH$_3$), 2.74 (m, 4H, CH$_2$), 7.0 (s, 1H, ArH).

2.3. Absorption and fluorescence spectroscopy

The UV/VIS and emission spectra were recorded on a Carl Zeiss Specord M400/M500 and a Bruins Instruments Omega 10 absorption spectrometer as well as a Spectronics Instruments 8100 spectrofluorometer. For the fluorescence experiments, only dilute solutions with an optical density (OD) below 0.01 at the excitation wavelength (OD<0.04 at the absorption maximum) were used. The relative fluorescence quantum yields (ϕ_f) were determined by adjusting the optical densities of the solutions at the excitation wavelengths to 0.1±0.001 in a 100 mm absorption cell. These solutions were then transferred to a 10 mm quartz cell and the fluorescence measurements were performed with a 90° standard geometry and excitation and emission polarizer set at 0 and 54.7°. Quinine sulfate in 1 N H$_2$SO$_4$ (ϕ_f=0.55±0.03, [37]), coumarin 1 in ethanol (ϕ_f=0.5, [38]), coumarin 153 in ethanol (ϕ_f=0.4, [38]), fluorescein 27 in 0.1 N NaOH (ϕ_f=0.90±0.03, [39]), DCM in methanol (ϕ_f=0.43±0.08, [40]), rhodamine 101 in ethanol (ϕ_f=1.00±0.02, [41]), and cresyl violet in methanol (ϕ_f=0.54±0.03, [41]) were used as fluorescence standards. All the fluorescence spectra presented here are corrected for the spectral response of the detection system (calibrated quartz halogen lamp placed inside an integrating sphere; Gigahertz–Optik) and for the spectral irradiance of the excitation channel (calibrated silicon diode mounted at a sphere port; Gigahertz–Optik). The fluorescence quantum yields were calculated from multiple measurements (N=6) and the uncertainties of the measurement were determined to ±5% (for ϕ_f>0.2), ±10% (for

0.2>ϕ_f>0.02), ±20% (for 0.02>ϕ_f>5×10^{-3}), and ±30% (for 5×10^{-3}>ϕ_f), respectively.

2.4. Complex stability constants

Most of the complex stability constants reported here were already published in [29] and the remaining values were determined from absorption measurements (in 50 or 100 mm absorption cells) by titrating a dilute solution (typically 10^{-6} M) of ligand by adding aliquots of metal ion solution (c_{M0}-titration). In the case of the hemicyanine and styryl probes, the complexometric titration data were fitted employing Eq. (4) derived from Eqs. (1)–(3) which apply to weak complexes where full complexation (A_{lim}) could not be reached (A — absorption intensity; a, b — constants; c_M, c_L, c_{ML} — free metal, free ligand, and complex concentrations, c_{Y0} — total concentrations, [13]).

$$K = \frac{c_{ML}}{c_L c_M} \tag{1}$$

$$A_0 = a c_{L0}, \qquad A_{lim} = b c_{L0}, \qquad \text{and}$$
$$A = a c_L + b c_M \tag{2}$$

$$c_{L0} = c_L + c_{ML} \qquad \text{and} \qquad c_{M0} = c_M + c_{ML} \tag{3}$$

$$\frac{A_0}{A - A_0} = \frac{a}{b - a} \frac{1}{K} c_M + 1 \tag{4}$$

For the complexes of the styryl bases showing high stability constants, Eq. (5) derived by Bourson et al. was used to fit the data [42].

$$A = A_0 + \frac{A_{lim} - A_0}{2 c_{L0}}$$
$$\times \left\{ c_{L0} + c_{M0} + \frac{1}{K_S} - \left[\left(c_{L0} + c_{M0} + \frac{1}{K_S} \right)^2 - 4 c_{L0} c_{M0} \right]^{1/2} \right\} \tag{5}$$

The reported values are mean values of at least two measurements with correlation coefficients >0.99.

3. Results and discussion

3.1. Uncomplexed hemicyanine dyes

3.1.1. Spectroscopic properties
The spectroscopic data of **1**–**4** in acetonitrile are collected in Table 1. All the hemicyanine dyes show a characteristic red-shifted narrow absorption band with a vibronic shoulder on the high energy side (ca. 1300 cm^{-1}) and a corresponding, only slightly Stokes-shifted emission band of mirror image shape. As an example, the spectra of **4a** and **4b** are shown in Fig. 1. As has recently been reported for the dimethylamino analogues of **1**–**3** in ethanol [31], the absorption spectra of the largely bridged compounds (**b**-series) are

Table 1
Spectroscopic properties of the hemicyanines **1–4** and their Ca^{II} complexes in acetonitrile at room temperature

	$\tilde{v}$ (abs) 10^3 cm^{-1}	FWHM cm^{-1}	$\tilde{v}$ (em) 10^3 cm^{-1}	FWHM cm^{-1}	$\Delta\tilde{v}$ (St) cm^{-1a}	ϕ_f	$\Delta\tilde{v}_{cp-fp}$ cm^{-1b}	$\log K_S$
1a	17.09	1150	16.34	980	750	0.100	–	–
1a⊂Ca^{II}	19.60	–	16.31	–	3290	0.058[c]	2510	0.94
1b	17.03	840	16.56	760	470	0.032	–	–
1b⊂Ca^{II}	n.d.[d]	–	–	–	–	–	–	–
1c	16.81	940	16.29	790	520	0.020	–	–
1c⊂Ca^{II}	20.67	–	16.27	–	4400	0.009 [c]	3860	1.41
2a	18.20	1200	17.33	1160	870	0.109	–	–
2a⊂Ca^{II}	20.43	–	17.32	–	3110	0.071[c]	2230	1.10
2b	17.86	780	17.48	790	380	0.075	–	–
2b⊂Ca^{II}	n.d.	–	–	–	–	–	–	–
3	17.35	1370	16.49	1150	860	0.072	–	–
3⊂Ca^{II}	n.d.	–	–	–	–	–	–	–
4a	16.55	1340	15.80	1070	750	0.060	–	–
4a⊂Ca^{II}	19.98	–	15.81	–	4170	0.025[c]	3430	1.36
4b	16.55	900	16.08	770	470	0.013	–	–
4b⊂Ca^{II}	n.d.	–	–	–	–	–	–	–

[a] Stokes shift.
[b] Shift in absorption between complexed and free probe.
[c] Determined at a 4×10^5-fold excess of Ca(ClO$_4$)$_2$ because full complexation could not be reached.
[d] No complex detectable.

slightly shifted to lower energies and show a reduced bandwidth (full width at half maximum, FWHM, in Table 1) as compared to the unbridged derivatives. Most probably, the decreased number of different ground state conformers for an increasingly rigidized molecular skeleton (**1a**→**1c**→**1b**) accounts for this behavior. This is also supported by photophysical studies of an unbridged symmetrical cyanine dye carried out recently by Noukakis et al. [43]. Depending on solvent polarity, these researchers found a nonexponential fluorescence decay behavior as well as a dependence of the time-resolved emission spectra on excitation wavelength and attributed this behavior to the presence of different isomeric species in the ground and excited state [43]. Consequently, **1c** carrying the *neo*-pentylene bridge shows intermediate bandwidths in both absorption and emission (Table 1).

The fluorescence quantum yields are generally weak to moderate ($0.013<\phi_f<0.115$) and do not increase with increasing rigidity of the molecular skeleton (Table 1). On the

contrary, in accordance with the studies of the dimethylamino analogues of **1a**–**1c** [31], the dye with two bridged bonds (**1c**) shows the weakest fluorescence. Such a reduction in fluorescence emission with bridging has also been reported for some *neo*-pentylene bridged symmetrical cyanine dyes compared to their unbridged analogues [44].

3.1.2. Photophysical mechanism

On the basis of the loose bolt theory [45,46] bridging should increase the fluorescence quantum yield. This anomalous 'inverse-loose-bolt' behavior, found here for the pairs of **1a** and **1b**, **2a** and **2b**, and **4a** and **4b**, is also observed for other pairs of compounds such as, e.g., the dimethylamino analogues of **2a** and **2b** [31]: in all cases, the emission of the unbridged derivative shows the higher quantum yield (Table 1). Following a theoretical concept recently put forward by Dekhtyar et al. for the reactivity of certain bonds in an ionic polymethine chain [47], an explanation involving the competing population of emissive and nonemissive twisted conformers during the lifetime of the excited state is anticipated [31,47]. For illustration, let us assume, as supported by the calculations [47], that twisting of some bonds in the hexamethine chain showing a stronger double bond character (these bonds are formally identical with the double bonds in the mesomeric structures given in Scheme 1) leads to the formation of a nonemissive state P* (formally connected with *trans–cis* photoisomerization) and passage through a photochemical funnel connecting S$_1$ with S$_0$ [48]. Transition from the initially excited all-planar conformation E* to P* thus leads to fluorescence quenching. Other twisted conformations accessible by rotation around a (formal) single bond can show emissive properties [49]. Keeping in mind
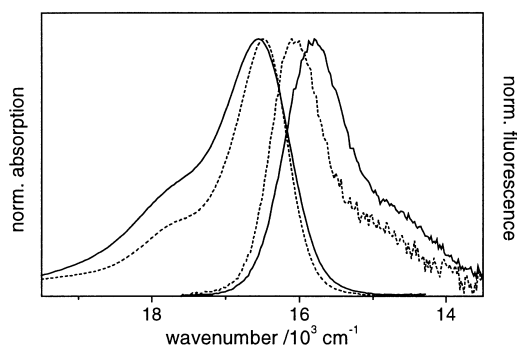

Fig. 1. Normalized steady-state absorption and emission spectra of **4a** (solid line) and **4b** (dotted line) in acetonitrile.

that the bonds most active with respect to P* formation in these molecules are located towards the chain's end [47] and that the second flexible bond adjacent to the heteromacrocyclic moiety was identified as the most prominent candidate for reaching P*, the behavior of the dyes studied here can be understood within this framework. For **1b**, **2b**, and **4b**, rotation around the most active second bond leads to more efficient P* state formation and thus to reduced fluorescence quantum yields as compared to **1a**, **2a**, and **4a** where a larger number of emissive species can also be populated by twisting around (formal) single bonds thus competing with formation of P*, the 'photochemical funnel', in the latter three molecules (Note that rotation of the first bond in the polymethine chain was found to be highly improbable [47].). However, the further reduced fluorescence of **1c** as compared to **1b** is still unclear and needs additional theoretical treatment, e.g., on the basis of investigations carried out for other fluorescent cyanine dyes [50].

3.2. Ca^{II} complexes of hemicyanine dyes

3.2.1. Ca^{II}-induced effects in absorption

The complexation-induced spectroscopic changes are also different for the certain types of bridged hemicyanine dyes, the data being included in Table 1. Whereas in the case of the unbridged molecules **1a**, **2a**, and **4a** as well as intermediately bridged **1c**, binding of Ca^{II} gives rise to a new blue-shifted and largely hypochromic absorption band, no such band is detected for the more strongly bridged compounds **1b**, **2b**, and **4b** as well as for unbridged **3**, even at a high excess of Ca^{II} (up to 4×10^5-fold). For a better comparison, all the spectra of the uncomplexed and complexed dyes of the **1**-series are combined in Fig. 2 illustrating the absence of the complexation-induced band at around $21\,000\,\mathrm{cm}^{-1}$ for **1b**. When complexation takes place the presence of this band
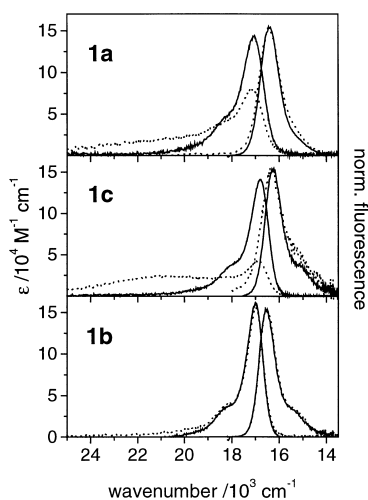

Fig. 2. Steady-state absorption and normalized emission spectra of **1a** (top), **1c** (middle), and **1b** (bottom) in acetonitrile in the absence (full line) and presence (dotted line) of a 4×10^5-fold excess of Ca(ClO$_4$)$_2$.

leads to sharp isosbestic points (at the crossing points of the spectra in Fig. 2) in a UV/VIS-spectrophotometric titration indicating the formation of well-defined 1:1-complexes.

The generally weak complexation ability can be understood in terms of the resonance interaction and distribution of the positive charge within the whole molecule [22,23,51]. With a low charge density at the crown ether nitrogen atom, complex formation has to overcome the weak affinity between receptor and cation.

Moreover, the lack of any detectable complexation in the case of the largely bridged compounds **1b**, **2b**, and **4b** cannot be explained purely on the basis of electronic interactions such as the charge at the crown ether nitrogen atom or repulsive forces between receptor and ion. Applying the empirical formalism recently developed for a correlation of $\log K_S$ and the charge of the dimethylamino group of the probe's dimethylamino analogue (Eq. (6), [29]), complexation is predicted for all three compounds as well. Fully optimizing the ground-state geometries of the dimethylamino analogues of **1b**, **2b**, and **4b** employing AM1 calculations [52] using an AMPAC package [53], values of 0.200 (**1b**), 0.219 (**2b**), and 0.186 (**4b**) were obtained for Q_{DMA} (Q_{DMA} is the sum of the net charges of N, C and H atoms contained in this dimethylamino group.). Applying Eq. (6), the corresponding theoretical $\log K_S$ of 1.36 (**1b**), 1.03 (**2b**), and 1.60 (**4b**) are calculated which are not much weaker than for the unbridged compounds (Table 1) but no Ca^{II}-induced changes are found in the absorption spectra of these ionophores.

$$\log K_S = 4.8 - 17.2 Q_{\mathrm{DMA}} \qquad (6)$$

However, the absence of cation-nitrogen interaction is verified by the fact that protonation leads to a drastic hypso- and hypochromic shift of the absorption band similarly for all three molecules **1a**, **1b**, and **1c**. Thus, other factors such as, for instance, sterical hindrance induced by the bridge must account for the lack of coordination of Ca^{II} with **1b**, **2b**, and **4b**. Such an explanation is supported by experimental and theoretical results obtained for DMABN and two of its crowned derivatives, DMABN-crown4 and DMABN-crown5 (Scheme 2) [54]. Here, the ratio of twisted intramolecular charge transfer (TICT) and locally excited (LE) emission, $\phi_f^{\mathrm{TICT}}/\phi_f^{\mathrm{LE}}$, increases in the order of DMABN<DMABN-crown4<DMABN-crown5 [54]. For this compound family, the enhanced TICT fluorescence correlates with an increased pretwist of the crown out of the molecular plane while maintaining a similar degree of pyramidalization of the crown ether nitrogen atom in all three compounds [54]. Thus, population of the TICT state is most easily achieved in DMABN-crown5 [54]. Moreover, this effect accounts for the weak complexing ability of DMABN-crown5 [54] as compared to closely related compounds such as DCS-crown or DS-crown (Scheme 2, [26]). In the case of the hemicyanines of the **b**-series showing very low $\log K_S$, such a further reduction in the complex stability constant would require a higher excess of metal salt to induce measureable spectroscopic effects and thus,
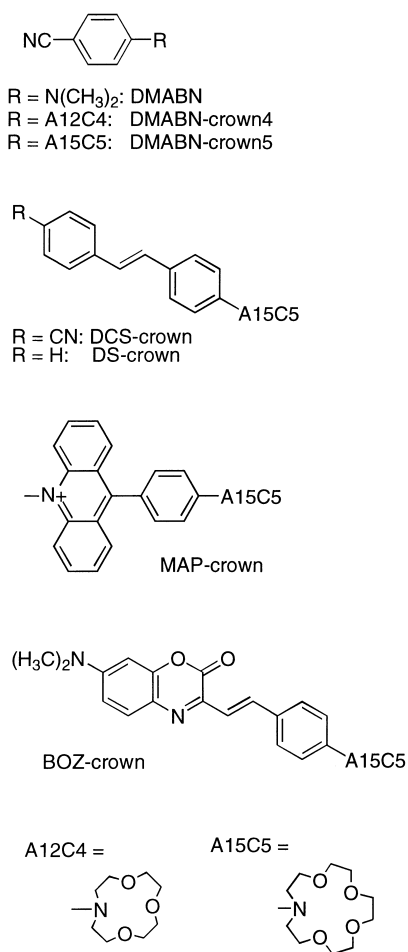
Scheme 2. Chemical structures of related dyes: DMABN and its crowned derivatives [54], DCS-crown and DS-crown [26], MAP-crown [62], and BOZ-crown [13].

the detection of a complex would be hampered by solubility problems.

3.2.2. Ca^{II}-induced effects in emission

The pronounced differences between the cation-induced shifts in absorption and emission for **1a**, **1c**, **2a**, **4a**, and their Ca^{II} complexes, are most probably due to the charge redistribution which takes place in the excited state. For asymmetric cyanines such as **1-4**, the polymethinic character increases in the excited state [51] and any twisting motion along the chain can promote such a charge redistribution in the excited state due to a formal transfer of the positive charge to one group only [47]. Accordingly, the immediate neighborhood of positively charged crown ether nitrogen atom and cation leads to a decoordination or recoordination reaction. Such features have been intensively studied for charged or neutral ICT probes [25–28,55] and the reader is referred to those works for a more detailed discussion.

Concerning the cation-induced fluorescence quenching observed, the mechanism remains unclear at present. Although full complexation could not be reached during the titration experiments, the fluorescence quantum yields given in Table 1 were obtained by exciting the complex at 460 nm, a region where the absorption of the free probe is negligible. Thus, with the data given in Table 1 for the high $Ca(ClO_4)_2$ excess, quenching factors of ca. 2 are obtained regardless of acceptor moiety or bridging pattern (with the exception of the dyes of the **b**-series). Concerning particular rotational motions in the excited state (e.g., around polymethinic 'single' or 'double' bonds), the increased bulkiness of the complexed 'cation-in-the-crown' moiety is expected to slow down all rotations but particularly decelerate the geometrical rearrangements leading to the formation of P* conformers [10]. Reduced population of P* species should yield higher fluorescence quantum yields, but no such cation-induced fluorescence enhancement is found. Moreover, when considering the total quenching of fluorescence by protonation of the hemicyanine dyes, distortions imposed on the charge distribution by complexation, i.e., electrostatic interaction between cation and nitrogen atom and thus a change in the relative energetic positions of species involved in an excited state reaction, seem to be a more probable explanation.

3.3. Uncomplexed styryl dyes

The styryl dyes investigated here comprise the positively charged stilbene analogues **6–9** and their spectroscopic properties are summarized in Table 2. The spectroscopic characteristics and cation complexation behavior of **5a** and **5b** have recently been published in ref. [11]. In accordance with the triad principle put forward by Dähne et al. [22,23,56], introduction of an aromatic structure in a (asymmetric) polymethine chain (e.g., **6** as compared to **4a**) shifts the absorption spectra to higher energies [57]. Furthermore, both the absorption and emission spectra of the styryl dyes are broad and structureless and the Stokes shifts observed are more pronounced (cf. data in Tables 1 and 2). This behavior is typical for so-called intrinsic ICT fluorescent probes where a charge transfer process takes place in the excited state from the crown donor fragment to the electron deficient acceptor subunit [2,3]. The charge redistribution taking place in these molecules usually leads to an increased dipole moment in the excited state and thus, in highly polar solvents such as acetonitrile, the excited state is more strongly stabilized than the ground state and large Stokes shift can be found [21].

But again, the fluorescence quantum yields are comparatively low, especially in the case of the acridinium- and the pyrylium-substituted dyes **7** and **9** (Table 2). Owing to the flexibility of the molecular skeleton and the charge transfer taking place in such molecules upon excitation [58], these photophysical properties can be understood within the framework of the biradicaloid charge transfer states [49]. Stabilization of such a charge transfer state is best achieved by orbital decoupling (twisting) of donor and acceptor moiety because in the twisted conformations the dipole moment achieves an extreme value [49]. Furthermore, these relaxation pathways can lead to emissive [59,60] or nonemissive

Table 2
Spectroscopic properties of the sytyrl dyes **6–9** and their Ca^{II} complexes in acetonitrile at room temperature

	$\tilde{v}$ (abs) 10^3 cm^{-1}	FWHM cm^{-1}	$\tilde{v}$ (em) 10^3 cm^{-1}	FWHM cm^{-1}	$\Delta\tilde{v}$ (St) cm^{-1a}	ϕ_f	$\Delta\tilde{v}_{cp-fp}$ cm^{-1b}	log K_S
5a	17.42	4620	12.33	1670	5090	0.130	–	–
5a⊂Ca^{II}	21.50	–	12.41	–	9090	0.032	4080, 80	3.12
6	18.87	3060	16.27	1960	2600	0.029	–	–
6⊂Ca^{II}	23.53	–	16.46	–	7070	0.010	4660, 190	2.21
7	15.81	3680	13.50	2740	2310	2×10^{-5}	–	–
7⊂Ca^{II}	21.33	–	14.29	–	7040	3×10^{-4}	5520, 790	2.88
8a	20.37	3280	14.96	2690	5410	0.021	–	–
8a⊂Ca^{II}	26.61	–	15.28	–	11330	0.072	6240, 320	2.90
8b	20.82	4010	14.02	3790	6800	2×10^{-3}	–	–
8b⊂CaII	26.67	–	14.90	–	11770	7×10^{-3}	5850, 880	2.82
9	15.92	2420	13.69	2330	2230	6×10^{-4}	–	–
9⊂Ca^{II}	20.88	–	14.07	–	6810	4×10^{-3}	4960, 380	1.96

[a] Stokes shift.

[b] Shift in absorption, emission between complexed and free probe.

[61,62] single-bond-twisted species in addition to the non-radiative decay via a so-called photochemical funnel, a double-bond-twisted species P* as discussed above [49,60]. It seems that in the styryl dyes **6–9**, in addition to the nonradiative channel P*, nonemissive single-bond-twisted species gain importance [60,63]. This is well supported by a preliminary study of bridged derivatives of the dimethyl-lamino analogue of **8a** [64,65]. A similar conclusion was reached for acridinium-type donor–acceptor-substituted biaryls lacking the central –CH=CH- group (MAP-crown, Scheme 2), where a nonemissive single-bond-twisted intramolecular charge transfer state has been proposed to account for efficient fluorescence quenching [62].

3.4. Ca^{II} complexes of styryl dyes

The step from the more (unsymmetrical cyanines **1–4**) to the less ideal polymethinic state (styryl dyes **5–9**) is reflected by the Ca^{II} binding properties, i.e., the styryl probes, although positively charged, show higher complex stability constants than the hemicyanine probes (log $K_S \sim 2.5$ in Table 2 compared to log $K_S \sim 1.1$ in Table 1). Thus, complex formation is observed for all the styryl probes (for **5b** see ref. [11]). On the other hand, the tendencies of the cation-induced shifts in both absorption and emission are comparable for both groups of positively charged dyes (large shifts in absorption and small shifts in emission, Table 2), the absolute shifts being approximately twice as large for **5–9** than for **1–4**. Again, sharp isosbestic points are observed in all cases pointing to a stoichiometry of 1:1 in the complexes. As an example, a set of titration spectra for **8a**/Ca(ClO$_4$)$_2$ is depicted in Fig. 3.

The changes in fluorescence quantum yield upon cation coordination to the macrocycle comprise fluorescence quenching (for **5a** and **6**) as well as fluorescence enhancement (for **7–9**), but the fluorescence enhancement or quenching factors are comparatively small. A similar behavior is observed for most other ionic ICT probes, i.e., for some probes fluorescence quenching is observed [8,66],
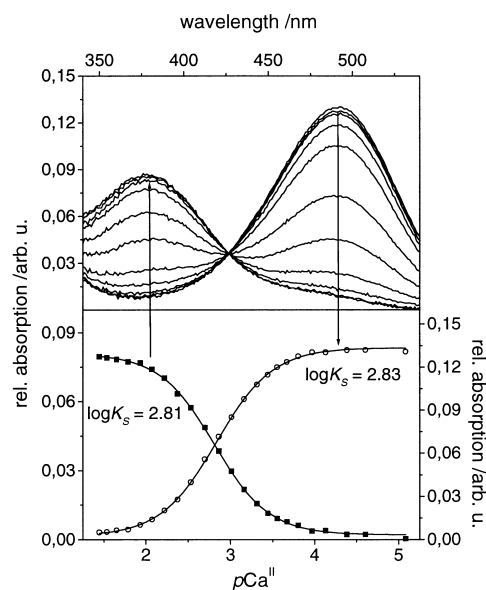

Fig. 3. UV/VIS-spectrophotometric titration spectra (top) and titration curves (bottom) of **8a** and Ca(ClO$_4$)$_2$ in acetonitrile ($c_{probe}=1\times10^{-6}$ M). The titration curve marked with ■ symbols (fit: —) corresponds to the increase in absorption at 380 nm and the curve marked with ○ (fit:- - -) corresponds to the decrease in absorption at 490 nm (isosbestic point at 426.5 nm). The complex stability constants obtained by the fit are indicated in the plot.

for others fluorescence enhancement was reported [6,10], and for some probes the change in fluorescence yield is even cation dependent [55]. Until today, the mechanisms accounting for these quantum yield changes remain largely obscure. Whereas the excited state recoordination reaction takes place on the fs to ps time scale, rotations around certain flexible bonds in the resultant excited state are not specifically inhibited by coordination in the crown ether receptor unit although the actual velocity of different rotations may change [10] (see also Section 3.2.2). Thus, most probably, comparatively small changes in the relative energetic positions of emissive or nonemissive states in the

excited complex (compared to the excited free dye) seem to be responsible for the delicate enhancement or quenching reaction. In the case of the above mentioned acridinium aniline crown studied by Jonker et al. only Ag^I complexation leads to a state inversion (the quenching state of the twisted conformation is now higher in energy) and partly restores fluorescence (ca. 7-fold enhancement) [62]. Possibly, a similar mechanism is responsible for the fluorescence enhancement in $7 \subset Ca^{II}$ (Note that the relatively large fluorescence enhancement factors FEF found for **7** (FEF=15) or **9** (7) have to be considered carefully since the error of the determination of fluorescence quantum yields in the range $<5 \times 10^{-3}$ is comparatively large, see Section 2.).

3.5. Uncomplexed styryl bases

Table 3 summarizes the spectroscopic properties of the fluorescent styryl base probes **10–14** and their Ca^{II} complexes. Compared to the corresponding ionic styryl dyes **8a** and **8b**, **10a** and **10b** contain a relatively electron rich acceptor, and the reduced CT character is manifested in blue-shifted absorption bands (ca. $6000 \, cm^{-1}$). Accordingly, excitation of the styryl bases again leads to an ICT reaction resulting in a largely Stokes-shifted emission (Table 3). The fluorescence quantum yields of the uncomplexed probes are moderate (**10a**, **11**, **12**, **13**) to considerably high (**10b**, **14**). The excited state reaction mechanisms accounting for fluorescence emission and losses are closely related to the photophysics of stilbene [67,68], benzoxazinone [13,69], or benzodiazinone dyes [16], with an all-flexible vinylene spacer between donor and acceptor. Since only spectroscopic investigations as a function of solvent polarity and temperature allow to draw conclusions on the involvement

of certain excited state mechanisms [67,68], no detailed explanations can be given here. **14**, being closely related to a crowned benzoxazinone derivative (BOZ-crown, Scheme 2) investigated by Fery–Forgues et al. [13], shows comparable spectroscopic features with a twice as large fluorescence quantum yield in acetonitrile.

3.6. Ca^{II} complexes of styryl bases

As would be expected for uncharged derivatives of **8a** and **8b**, the complex stability constants ($\log K_S$) obtained for the Ca^{II} complexes of **10a** and **10b** are much higher than for the former two probes (4.57 versus 2.90 for **10a/8a** and 4.80 versus 2.82 for **10b/8b**). As expected, the values of $\log K_S$ of $11 \subset Ca^{II}$ and $12 \subset Ca^{II}$ are in the same range (Table 3). Even for both probes carrying a second dimethylamino (**13**) or julolidino (**14**) donor group in the acceptor part of the molecule (a D_1-A-D_2 constitution with D_2=crown), the complex stability constants are comparatively high ($\log K_S$=4.52 for $13 \subset Ca^{II}$ and 4.54 for $14 \subset Ca^{II}$).

3.6.1. Donor–acceptor-substituted styryl bases
The spectral shifts observed upon cation binding are again indicative of typical ICT probes for the D-A compounds **10–12**, i.e., large hypsochromic shifts in absorption and less pronounced effects but of the same tendency in emission (Table 3). Interestingly, complexation induces a second blue-shifted emission band for **10a** and **10b**. Following a spectrophotometric titration of **10a** or **10b** with $Ca(ClO_4)_2$ well defined isosbestic points are observed. On the other hand, exciting the complex at 340 nm yields an emission spectrum composed of two bands (Fig. 4). Inspection of the fluorescence excitation spectra reveals different excita-

Table 3

Spectroscopic properties of the sytyrl bases **10–14** and their Ca^{II} complexes in acetonitrile at room temperature

	$\tilde{v}$ (abs) $10^3 \, cm^{-1}$	$\tilde{v}$ (em) $10^3 \, cm^{-1}$	$\Delta\tilde{v}$ (St) $cm^{-1 \, a}$	ϕ_f	$\Delta\tilde{v}_{cp-fp} \, cm^{-1 \, b}$	$\log K_S$
10a	26.28	19.77	6510	0.082	–	–
$10a \subset Ca^{II}$	30.86	20.29	10570	0.120	4580, 520	4.57[c]
	32.05[d]	25.60	6450	n.d.[e]	5770, 5830	n.d.
10b	26.13	18.82	7380	0.220	–	–
$10b \subset Ca^{II}$	28.74	19.53	9210	0.250	2610, 780	4.80[c]
	29.41[d]	22.95	6460	n.d.	3280, 4200	n.d.
11	27.73	21.45	6280	0.021	–	–
$11 \subset Ca^{II}$	31.85	22.01	9840	0.037[f]	4120, 560	4.44
$[11 \subset Ca^{II}]Ca^{II}$	27.03[d]	16.45	10580	n.d.	−920, −5000	n.d.
12	24.45	18.89	5560	0.011	–	–
$12 \subset Ca^{II}$	27.70	20.15	7190	0.017	3250, 1620	4.44
13	24.45	19.63	4820	0.027	–	–
$13 \subset Ca^{II}$	25.12	18.24	6700	0.86	670, −1210	4.52
14	19.48	15.86	3620	0.64	–	–
$14 \subset Ca^{II}$	19.90	16.70	3190	0.77	420, 850	4.54

[a] Stokes shift.
[b] Shift in absorption, emission between complexed and free probe.
[c] Obtained in the longest wavelength absorption band where only the *trans* isomer absorbs.
[d] Maximum of the corresponding fluorescence excitation spectrum.
[e] Not determined.
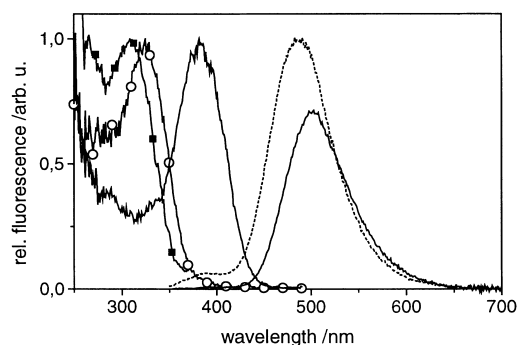[f] At full complexation in the crown (500-fold Ca^{II} excess).

Fig. 4. Fluorescence spectra of **10a** and **10a⊂Ca^{II}** in acetonitrile (c_{probe}=1×10^{-6} M). Solid lines: spectra of free **10a** (excited at 380 nm, observed at 500 nm); dotted line: emission spectrum of **10a⊂Ca^{II}** (excited at 340 nm); ■: excitation spectrum of **10a⊂Ca^{II}** (recorded at 380 nm), ○: excitation spectrum of **10a⊂Ca^{II}** (recorded at 500 nm). The fluorescence excitation spectra are normalized for a better comparison.

Fig. 5. UV/VIS-spectrophotometric titration spectra of **11** and Ca(ClO$_4$)$_2$ in acetonitrile (c_{probe}=1×10^{-6} M). The titration curve marked □ corresponds to free **11**, the curve marked ● was recorded at an 790-fold Ca^{II} excess. The changes in the bands and the ratios of Ca^{II} : **11** are indicated in the plot.

tion spectra for both emission bands (Fig. 4). But when the Ca^{II}-induced decrease of the low energy absorption band is fitted to Eq. (6) (see Section 2), a satisfactory fit for a 1:1-complex is obtained (see log K_S in Table 3) and no hints for the formation of a complex of higher order or stoichiometry is found. As will be shown below for the Ca^{II} complex of **11**, binding of a second calcium ion to the pyridino nitrogen atom in the acceptor part of the molecule would result in bathochromic shifts, especially in emission as a consequence of the increased charge density on the pyridine ring in the excited state, and is very unlikely to be the cause of the behavior observed for **10a** and **10b**, i.e., blue-shifted fluorescence emission and (corresponding) excitation spectra. A possible explanation might involve the formation of *trans* and *cis* complex isomers (with comparable log K_S), since both the fluorescence emission and excitation spectra of the second species are blue-shifted (Fig. 4). However, with the methods employed here, the nature of the two complex species could not be elucidated.

In the case of **11**, sharp isosbestic points are observed during a spectrophotometric titration in the whole absorption range measured (220–500 nm, Fig. 5). Monitoring a fluorometric titration, up to a ca. 2500-fold excess of Ca^{II} a slight hypsochromic shift accompanied by an increase in intensity is observed as would be expected for a 1:1 complexation of an ICT probe (upper part in Fig. 6). But a further increase in ion concentration leads to the appearance of a second red-shifted emission band, i.e., dual emission is observed (No red-shifted bands are found for **10a** and **10b** even at a very high (3×10^5-fold) ion excess.).

Taking a look at the corresponding fluorescence excitation spectra the dual emission behavior is identified as linked to different ground state species. The bathochromically emitting species shows a fluorescence excitation spectrum centered at nearly the same wavelength as that of the free dye (370 nm compared to 361 nm, Table 3 and Fig. 7). Inspecting the spectrophotometric titration spectra in that concentration range reveals the appearance of a weak shoulder in the
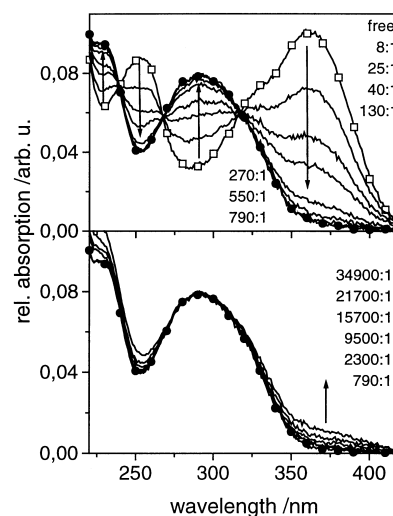
same wavelength region (lower part in Fig. 5). Thus, a second strongly fluorescent species must be present in solution. Loose coordination of a second Ca^{II} ion to the pyridino nitrogen atom seems to account for the spectroscopic features of this second species observed only at a very high ion excess. Such a coordinating ion would increase the acceptor strength and could outbalance the weakened 'ion-in-the-crown' complexed donor. Accordingly, the absorption band of such a species would be shifted to lower energies as compared to the 1:1-complex. Upon excitation and CT reaction, the bond between crown ether nitrogen atom and the cation in the
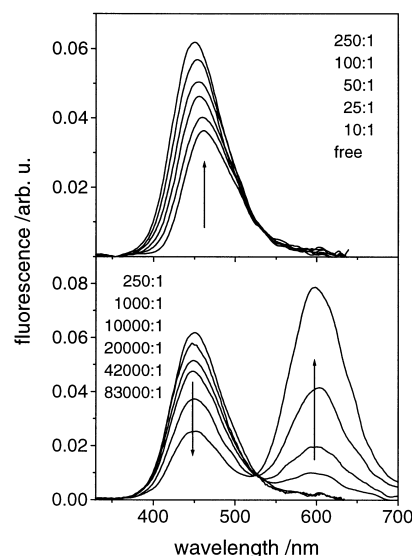

Fig. 6. Fluorometric titration spectra of **11** and Ca(ClO$_4$)$_2$ in acetonitrile (c_{probe}=1×10^{-6} M; excited at the isosbestic point at 318 nm, s. Fig. 5). The titration steps and changes in the bands are indicated in the plot. The figures denote the Ca^{II}-to-probe ratios.
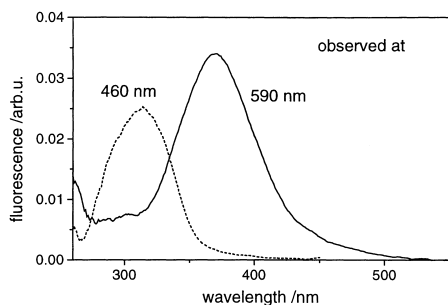
Fig. 7. Fluorescence excitation spectra of an acetonitrile solution containing **11** ($c_{probe}=1\times10^{-6}$ M) and a 42000-fold excess of Ca(ClO$_4$)$_2$ recorded at 460 nm (dotted line) and 590 nm (solid line).

Fig. 8. Steady-state absorption and normalized emission spectra of free and complexed **13** (top) and **14** (bottom) in acetonitrile (free probe ○, complex ■; excitation at the absorption maximum).

crown is weakened (i.e., CT-induced cation decoordination takes place, [25–28]) but on the other hand the bond between the pyridino nitrogen atom and the second cation is strengthened. Accordingly, writing **11** as **A-11-D**, the main absorbing and emitting species can schematically be characterized by Ca^{II}[**A-11-D**⊂Ca^{II}] and ([Ca^{II}⊃**A-11-D**]Ca^{II})* where the more strongly coordinated Ca^{II} is indicated by the horseshoe. The resulting effect is an extraordinary large Stokes shift (M:L-complex: 9840 cm^{-1}, M$_2$:L-complex: 10580 cm^{-1}). This is not observed for **10a** and **10b**. Apparently, the phenyl groups adjacent to the pyridino nitrogen in **10a** and **10b** prevent coordination of a second ion.

The slight increase in emission yield observed for **10–12** upon binding of Ca^{II} is very similar to effects found for a series of related stilbene [13,15,16] or merocyanine crowns [14] and a mechanistic explanation should involve the factors given above for the styryl probes.

3.6.2. Donor–acceptor-donor-substituted styryl bases

In contrast to the typical ICT probe behavior, for **13** and **14**, different changes are observed upon cation binding. In accordance with the results obtained by Fery–Forgues et al. for BOZ-crown [13], the D$_1$-A-D$_2$ probes show comparatively small shifts upon complexation. Whereas **14** behaves very much the same as BOZ-crown (showing small hypsochromic shifts [13]), for **13** a bathochromic shift is observed in emission (Fig. 8).

Even more interestingly, in the case of **13**, an unusually strong fluorescence enhancement is observed (factor of 32, Table 3). Such large enhancement factors, commonly referred to as a 'switching on' of the fluorescence, are normally only observed for electron transfer probes with a decoupled donor–acceptor arrangement [4]. Assuming, that the mechanistical model put forward for the excited state reaction mechanism of BOZ dyes [13,69,70] and donor–donor-substituted stilbenes [17,71] is valid for **13** and **14** as well, differences in energy level positions of the potentially emissive states E* and A* and the potentially nonemissive state P* are most probably responsible for the effects found. This three-state-model is closely related to the models already outlined in Sections 3.1.2 and 3.3 and
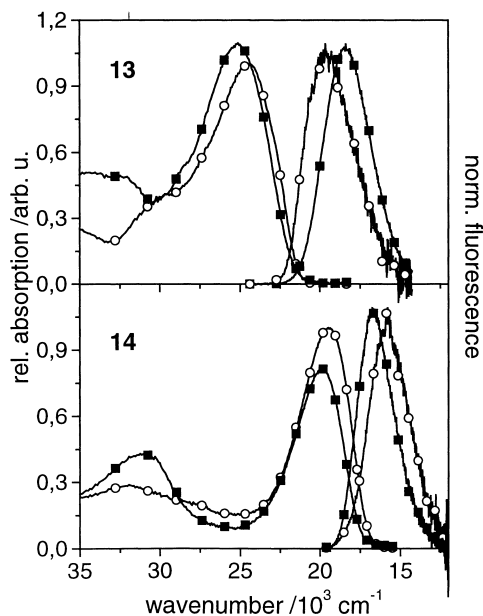
involves different excited conformers of planar or twisted nature [49,68,69]. For the bathochromically absorbing BOZ dyes as well as **14**, the emissive A* state is energetically much more favored in a highly polar solvent such as acetonitrile and the fluoroionophores are already strongly fluorescent in the uncomplexed state and **14**, like BOZ-crown, shows only a weak Ca^{II}-induced fluorescence enhancement of a factor of 1.2. For **13**, the energy differences between E*, P*, and A* states are less pronounced and more efficient quenching occurs in acetonitrile for the uncomplexed dye (Table 3). Upon complexation, the quenching reaction during the lifetime of the excited state is very effectively inhibited in **13** and fluorescence is nearly completely restored (ϕ_f [**13**⊂Ca^{II}]=0.86). Moreover, the red-shifted emission of **13**⊂Ca^{II} as compared to **13** suggests that the crowned anilino donor in **13** is turned into an acceptor upon complexation and the ICT process occurs mainly from the dimethylamino group directly bound to the benzothiazole moiety as observed for related D-A-A-substituted BOZ derivatives [70].

4. Concluding remarks

Several factors are important for the applicability of fluorescent probes in fluorometric analysis. Besides selectivity, (i) solubility in aqueous media or media which are miscible with water, (ii) absorption and emission in the NIR range of the spectrum (favorably with a large Stokes shift), (iii) drastic cation-induced spectroscopic changes, (iv) fluorescence enhancement instead of fluorescence quenching reactions upon complexation, (v) high complex stability constants, and

(vi) fast and reversible complexation reactions are highly desirable. Concerning (i), all the dyes investigated here are soluble in such media in the concentration range of interest ($<10^{-5}$ M). Carrying a monoaza tetraoxa crown ether receptor, point (vi) is also fulfilled for the probes studied. But comparing the data in Tables 1–3 it is obvious that points (ii) and (v) seem to exclude each other: The positively charged dyes, absorbing and emitting well in the visible or NIR region, show considerably lower complex stability constants than the neutral dyes absorbing at higher energy. This is especially hampering an analytical application in the case of the crowned hemicyanines **1**–**4**. Here, the small Stokes shift is another argument against a practical exploitation of this type of dyes. For the styryl probes **5**–**9**, showing NIR absorption and emission and moderate complex stability constants, the low (absolute) fluorescence quantum yield does not favor a straightforward application. Although the fluorescence enhancement factors of **7** and **9** are relatively high for 'classic' ICT probes (positive in terms of (iii) and (iv)), the low emission yield of the complex ($\phi_f < 0.005$) is critical. Concerning the important requirements (iii) and (iv), a sensible D_1-A-D_2 setup as in **13** seems to be most promising for further ICT probe design. Furthermore, the concept of bifunctional ionophores as exemplified by **11** possesses an enormous potential for the construction of new sensor molecules.

Acknowledgements

References

[1] H.-G. Löhr, F. Vögtle, Acc. Chem. Res. 18 (1985) 65.

[2] B. Valeur, in: J.R. Lakowicz (Ed.), Probe Design and Chemical Sensing, Plenum, New York, 1994, p. 21.

[3] W. Rettig, R. Lapouyade, in: J.R. Lakowicz (Ed.), Probe Design and Chemical Sensing, Plenum, New York, 1994, p. 109.

[4] A.P. de Silva, H.Q.N. Gunaratne, T. Gunnlaugsson, A.J.M. Huxley, C.P. McCoy, J.T. Rademacher, T.E. Rice, Chem. Rev. 97 (1997) 1515.

[5] A.V. Barzykin, M.A. Fox, E.N. Ushakov, O.B. Stanislavsky, S.P. Gromov, O.A. Fedorova, M.V. Alfimov, J. Am. Chem. Soc. 114 (1992) 6381.

[6] K.J. Thomas, K.G. Thomas, T.K. Manojkumar, S. Das, M.V. George, Proc. Ind. Acad. Sci. Chem. Sci. 106 (1994) 1375.

[7] N. Mateeva, V. Enchev, L. Antonov, T. Deligeorgiev, M. Mitewa, J. Inclusion Phenom. Mol. Recognit. Chem. 20 (1995) 323.

[8] M.V. Alfimov, A.V. Churakov, Y.V. Fedorov, O.A. Fedorova, S.P. Gromov, R.E. Hester, J.A.K. Howard, L.G. Kuz'mina, I.K. Lednev, J.N. Moore, J. Chem. Soc. Perkin Trans. 2 (1997) 2249.

[9] I.K. Lednev, R.E. Hester, J.N. Moore, J. Am. Chem. Soc. 119 (1997) 3456.

[10] I.K. Lednev, T.-Q. Ye, R.E. Hester, J.N. Moore, J. Phys. Chem. A 101 (1997) 4966.

[11] K. Rurack, J.L. Bricks, J.L. Slominskii, U. Resch-Genger, in: S. Dähne, U. Resch-Genger, O.S. Wolfbeis, (Eds.), Near-Infrared Dyes for High Technology Applications, NATO ASI Ser., Ser. 3, Vol. 52, Kluwer Academic, Dordrecht, 1998, p. 191.

[12] S.P. Gromov, Y.V. Fedorov, O.A. Fedorova, A.I. Vedernikov, A.V. Churakov, M.V. Alfimov, L.G. Kuz'mina, J.A.K. Howard, S. Bossmann, A. Braun, M. Woerner Jr, D.F. Sears, J. Saltiel, J. Am. Chem. Soc. 121 (1999) 4992.

[13] S. Fery-Forgues, M.T. Le Bris, J.-P. Guetté, B. Valeur, J. Phys. Chem. 92 (1988) 6233.

[14] J. Bourson, B. Valeur, J. Phys. Chem. 93 (1989) 3871.

[15] J.-F. Létard, R. Lapouyade, W. Rettig, Pure Appl. Chem. 65 (1993) 1705.

[16] L. Cazaux, M. Faher, A. Lopez, C. Picard, P. Tisnes, J. Photochem. Photobiol. A Chem. 77 (1994) 217.

[17] S. Delmond, J.-F. Létard, R. Lapouyade, R. Mathevet, G. Jonusauskas, C. Rullière, New J. Chem. 20 (1996) 861.

[18] K. Rurack, J.L. Bricks, A.D. Kachkovskii, U. Resch, J. Fluoresc. 7 (1997) 63S.

[19] A. Bolia-Göckel, H. Junek, J. Prakt. Chem. 341 (1999) 20.

[20] K. Rurack, J.L. Bricks, G. Reck, R. Radeglia, U. Resch-Genger, J. Phys. Chem. A, in press.

[21] W. Liptay, Z. Naturforsch. 20a (1965) 1441.

[22] S. Dähne, D. Leupold, Angew. Chem. Int. Ed. Engl. 5 (1966) 984.

[23] S. Dähne, F. Moldenhauer, Prog. Phys. Org. Chem. 15 (1985) 1.

[24] A.A. Ishchenko, Russ. Chem. Bull. 43 (1994) 1161.

[25] M.M. Martin, P. Plaza, N. Dai Hung, Y.H. Meyer, J. Bourson, B. Valeur, Chem. Phys. Lett. 202 (1993) 425.

[26] P. Dumon, G. Jonusauskas, F. Dupuy, P. Pée, C. Rullière, J.-F. Létard, R. Lapouyade, J. Phys. Chem. 98 (1994) 10391.

[27] R. Mathevet, G. Jonusauskas, C. Rullière, J.-F. Létard, R. Lapouyade, J. Phys. Chem. 99 (1995) 15709.

[28] M.M. Martin, P. Plaza, Y.H. Meyer, F. Badaoui, J. Bourson, J.-P. Lefevre, B. Valeur, J. Phys. Chem. 100 (1996) 6879.

[29] K. Rurack, M. Sczepan, M. Spieles, U. Resch-Genger, W. Rettig, Chem. Phys. Lett., submitted for publication.

[30] Gmelins Handbuch der Anorganischen Chemie. Chor, 8th Edition, VCH, Berlin, 1927.

[31] M. Sczepan, W. Rettig, Y.L. Bricks, Y.L. Slominski, A.I. Tolmachev, J. Photochem. Photobiol. A Chem. 124 (1999) 75.

[32] F.M. Hamer, The Cyanine Dyes and Related Compounds, Interscience, New York, 1964.

[33] Y.L. Slominski, A.L. Smirnova, S.V. Popov, A.I. Tolmachev, Zh. Org. Khim. 19 (1983) 2389.

[34] A.I. Tolmachev, N.A. Derevyanko, E.F. Karaban, M.H. Kudinova, Khim. Geterotsikl. Soedin. 5 (1975) 612.

[35] G.N. Dorofeenko, E.I. Sadekova, Preparative Chemistry of Pyrylium Salts, Rostov University Press, Rostov, 1972, p. 227.

[36] A.G. Balaban, C.T. Nenitzescu, Ann. 625 (1959) 74.

[37] J.N. Demas, in: K.D. Mielenz (Ed.), Optical Radiation Measurements, Vol. 3, Academic, New York, 1982, p. 195.

[38] K.H. Drexhage, J. Res. Natl. Bur. Stand. 80A (1976) 421.

[39] J. Olmsted III, J. Phys. Chem. 83 (1979) 2581.

[40] J.M. Drake, M.L. Lesiecki, D.M. Camaioni, Chem. Phys. Lett. 113 (1985) 530.

[41] D.F. Eaton, Pure Appl. Chem. 60 (1988) 1107.

[42] J. Bourson, J. Pouget, B. Valeur, J. Phys. Chem. 97 (1993) 4552.

[43] D. Noukakis, M. Van der Auweraer, S. Toppet, F.C. De Schryver, J. Phys. Chem. 99 (1995) 11860.

[44] R.C. Benson, H.A. Kues, J. Chem. Eng. Data 22 (1977) 379.

[45] G.N. Lewis, M. Calvin, Chem. Rev. 25 (1939) 273.

[46] L.J.E. Hofer, R.J. Grabenstetter, E.O. Wiig, J. Am. Chem. Soc. 72 (1950) 203.

[47] M. Dekhtyar, W. Rettig, V. Rozenbaum, J. Photochem. Photobiol. A Chem. 120 (1999) 75.

[48] F. Bernardi, M. Olivucci, M.A. Robb, Chem. Soc. Rev. 25 (1996) 321.

[49] W. Rettig, Top. Curr. Chem. 169 (1994) 253.

[50] P. Czerney, G. Graneß, E. Birckner, F. Vollmer, W. Rettig, J. Photochem. Photobiol. A Chem. 89 (1995) 31.

[51] A.D. Kachkovskii, Russ. Chem. Rev. 66 (1997) 647.

[52] M.J.S. Dewar, E.G. Zoeblich, E.F. Healy, J.J.P. Stewart, J. Am. Chem. Soc. 107 (1985) 3202.

[53] M.J.S. Dewar, J.J.P. Stewart, J.M. Ruiz, D. Liotard, E.F. Healy, R.D. Dennington II, AMPAC 5.0, (Semichem, Shawnee, 1994).

[54] J.-F. Létard, S. Delmond, R. Lapouyade, D. Braun, W. Rettig, M. Kreissler, Recl. Trav. Chim. Pays-Bas 114 (1995) 517.

[55] S.I. Druzhinin, M.V. Rusalov, B.M. Uzhinov, S.P. Gromov, S.A. Sergeev, M.V. Alfimov, J. Fluoresc. 9 (1999) 33.

[56] S. Dähne, K. Hoffmann, Prog. Phys. Org. Chem. 18 (1990) 1.

[57] N. Tyutyulkov, J. Fabian, A. Mehlhorn, F. Dietz, A. Tadjer, Polymethine Dyes, St. Kliment Ohridski University Press, Sofia, 1991, p. 141.

[58] X. Cao, R.W. Tolbert, J.L. McHale, W.D. Edwards, J. Phys. Chem. A 102 (1998) 2739.

[59] B. Strehmel, W. Rettig, J. Biomedical Opt. 1 (1996) 98.

[60] B. Strehmel, H. Seifert, W. Rettig, J. Phys. Chem. B 101 (1997) 2232.

[61] P. Plaza, N.D. Hung, M.M. Martin, Y.H. Meyer, M. Vogel, W. Rettig, Chem. Phys. 168 (1992) 365.

[62] S.A. Jonker, S.I. van Dijk, K. Goubitz, C.A. Reiss, W. Schuddeboom, J.W. Verhoeven, Mol. Cryst. Liq. Cryst. 183 (1990) 273.

[63] H. Ephardt, P. Fromherz, J. Phys. Chem. 93 (1989) 7717.

[64] M. Sczepan, W. Rettig, A.I. Tolmachev, J.L. Slominski, in: Book of Abstracts, VI International Conference on Methods and Applications of Fluorescence Spectroscopy, Paris, CNAM/CNRS, Paris, 1999, Abstract P63.

[65] W. Rettig, K. Rurack, M. Sczepan, in: B. Valeur, J.C. Brochon (Eds.), in: Proceedings of the Conference on Methods and Applications of Fluorescence Spectroscopy, Paris, 1999, Springer, Berlin, to appear in 2000.

[66] S.I. Druzhinin, M.V. Rusalov, B.M. Uzhinov, M.V. Alfimov, S.P. Gromov, O.A. Fedorova, Proc. Ind. Acad. Sci. Chem. Sci. 107 (1995) 721.

[67] W. Rettig, W. Majenz, Chem. Phys. Lett. 154 (1989) 335.

[68] J.-F. Létard, R. Lapouyade, W. Rettig, J. Am. Chem. Soc. 115 (1993) 2441.

[69] S. Fery-Forgues, M.-T. Le Bris, J.-C. Mialocq, J. Pouget, W. Rettig, B. Valeur, J. Phys. Chem. 96 (1992) 701.

[70] M.-T. Le Bris, J. Mugnier, J. Bourson, B. Valeur, Chem. Phys. Lett. 106 (1984) 124.

[71] J.-F. Létard, R. Lapouyade, W. Rettig, Chem. Phys. Lett. 222 (1994) 209.